A CONSTRAINT BASED APPROACH TO CORRELATE FRACTURE BEHAVIOR IN TEST SPECIMENS AND CRACKED PIPELINES

S. CRAVERO and C. RUGGIERI
Dept. of Naval Architecture and Ocean Engineering,University of São Paulo, SP 05508-900, Brazil

ABSTRACT

This work presents a numerical investigation of crack-tip constraint for SE(T) specimens and axially surface cracked pipes using plane-strain, nonlinear computations. The primary objective is to gain some understanding of the potential applicability of constraint designed fracture specimens in defect assessments of pressurized pipelines and cylindrical vessels. The present study builds upon the *J-Q* approach using plane-strain solutions to characterize effects of constraint on cleavage fracture behavior for fracture specimens and cracked pipes. Under increased loading, each cracked configuration follows a characteristic *J-Q* trajectory which enables comparison of the corresponding crack-tip driving force. The results provide a strong support to use constraint-designed SE(T) specimens in fracture assessments of pressurized pipes and cylindrical vessels.

1 INTRODUCTION

This work presents a numerical investigation of crack-tip constraint for SE(T) specimens and axially surface cracked pipes using plane-strain, nonlinear computations. The primary objective is to gain some understanding of the potential applicability of constraint designed fracture specimens in defect assessments of pressurized pipelines and cylindrical vessels. The analysis matrix considers SE(T) fracture specimens with varying geometries (*i.e.*, different notch depth to specimen width ratio, a/W, as well as different loading point distance, H), and test conditions (pin-loaded ends *vs*. clamped ends). The numerical models for the cracked pipes cover different notch depth to pipe wall thickness, a/t, ratios. The present study builds upon the *J-Q* approach using plane-strain solutions to characterize effects of constraint on cleavage fracture behavior for fracture specimens and cracked pipes. Under increased loading, each cracked configuration follows a characteristic *J-Q* trajectory which enables comparison of the corresponding crack-tip driving forces curve. The numerical results provide a strong support to use constraint-designed SE(T) specimens in fracture assessments of pressurized pipes and cylindrical vessels.

2 CORRELATION OF FRACTURE BEHAVIOR IN CRACKED COMPONENTS

The marked differences of toughness values (J_c, CTOD) for shallow crack and deep crack specimen geometries in ferritic steels at temperatures in the ductile-to-brittle transition (DBT) region underlie the loss of one-to-one correspondence between J and the elastic-plastic crack-tip fields; such loss

of a unique relationship between the crack tip fields and J under large scale yielding (LSY) conditions is most often referred to as *constraint loss*. O'Dowd and Shih (OS) [1,2] proposed a two-parameter description for the elastic-plastic crack tip fields based upon a triaxiality parameter more applicable under LSY conditions in the form

$$\sigma_{ij} = (\sigma_{ij})_{\text{SSY}} + Q\sigma_0\delta_{ij} \tag{1}$$

where σ_0 is the material's reference (yield) stress and the dimensionless second parameter Q defines the amount by which σ_{ij} in fracture specimens differ from the stress fields for a reference solution. A widely adopted approach employs stress fields constructed for plane-strain, small scale conditions (SSY) as the reference fields to define *relative* constraint differences. Consequently, Q is defined by

$$Q \equiv \frac{\sigma_{\theta\theta} - (\sigma_{\theta\theta})_{\text{SSY}}}{\sigma_0} \tag{2}$$

where the difference field is conventionally evaluated at the normalized crack-tip distance $r = 2J/\sigma_0$ which represents the location of the triggering cleavage mechanism ahead of crack tip. Construction of J-Q trajectories for structural components and fracture specimens then follows by the evaluation of Eq. (2) at each stage of loading in the finite body. At similar values of the continuum, scalar parameters (J, Q), the crack-tip strain-stress fields which drive the local process have similar values as well. Consequently, cracked bodies with similar J-Q trajectories or driving force curves exhibit similar conditions for cleavage fracture.

This work employs nonlinear finite element analyses conducted on plane-strain models for selected pin-loaded and clamped SE(T) specimens (which are denoted here as SE(T)$_P$ and SE(T)$_C$ specimens) and cracked pipes to evaluate Q by means of Eq. (2). The analysis matrix covers a wide range of SE(T) fracture specimens with varying geometry and crack sizes: $a/W = 0.1$, 0.25, 0.35, 0.5 and $H/W = 2$, 4, 6. Here, a is the crack size, W is the specimen width and H is the distance between the pin loading or clamps. Figure 1 shows the geometry for the analyzed SE(T) specimens. Plane-strain finite element analyses are also conducted on axially cracked pipes with $D = 508$ mm (20 in) and external surface flaws with different a/t-ratios: $a/t = 0.1$, 0.25, 0.5 and $D/t = 40$. Here, a is the crack depth, t is the pipe wall thickness and D is the pipe outside diameter. These geometries typify current trends in high pressure, high strength pipelines of increased diameters with reduced thickness.

The numerical computations reported here are generated using the research code WARP3D [3]. All finite element models have an adequate level of mesh refinement and employ a conventional mesh configuration having a focused ring of elements surrounding the crack front with a small key-hole at the crack tip; the radius of the key-hole, ϱ_0, is 2.5μm (0.0025 mm). The SSY reference fields used to evaluate Q by means of Eq. (2) are obtained from a plane-strain finite element analysis of an infinite domain, single-ended crack model under Mode I loading with the same mesh configuration at the crack tip. Cravero and Ruggieri [4] present further details of the numerical procedures employed. The analyses utilize an elastic-plastic constitutive model with J_2 flow theory and conventional Mises plasticity in small geometry change (SGC) setting using a simple power-hardening model to characterize the uniaxial true stress-logarithmic strain in the form $(\epsilon/\epsilon_0) = (\sigma/\sigma_0)^n$ for $\sigma > \sigma_0$, where σ_0 and ϵ_0 are the reference (yield) stress and strain, and n is the strain hardening exponent. The finite element analyses consider material flow properties covering a typical API X60 ~ X70 pipeline steel with $n = 10$ and $E/\sigma_0 = 500$. Here, $E = 206$ GPa and $\nu = 0.3$.

3 RESULTS AND DISCUSSION

3.1 J-Q Trajectories for SE(T) Specimens

Figures 1(a-b) compare the effect of loading conditions (pin-loaded end *vs.* clamped ends) for the SE(T) specimens with $H/W = 4$ and different a/W-ratios. The parameter Q is defined by Eq. (2) at $r = 2J/\sigma_0$ whereas J is normalized by $b\sigma_0$ with b denoting the remaining crack ligament $W - a$. Remarkably, the loading condition has a great effect on the J-Q trajectories for the SE(T) specimens. The pin-loaded specimens display strong dependence on crack size showing significant constraint loss with decreased a/W-ratio. In contrast, the clamped specimens display a relatively small dependence of J-Q trajectories on a/W-ratio. Here, a noteworthy feature of these results is that large constraint loss occurs for all a/W-ratios at low deformation levels, even for deeper crack specimens ($a/W = 0.35$ and 0.5).

The effect of H/W-ratio on J-Q trajectories for the SE(T) specimens with different a/W-ratios and $n = 10$ is presented in Figs. 2(a-b). While the J-Q trajectories displayed by these plots also depend strongly on loading conditions, the results reveal that the short crack specimens ($a/W = 0.1$) with both pin-load and clamped ends depend weakly on H/W-ratio, particular for the clamped specimen (Fig. 2(b)); for this specimen, the H/W-ratio has a negligible effect on the J-Q curves. In contrast, the deep crack SE(T) specimen with clamped ends (Fig. 2(b)) displays a much greater (relative) dependence on H/W-ratio; here, the deep crack specimen ($a/W = 0.5$) with $H/W = 2$ has constraint levels which are similar to those for the short crack SE(T) specimens with clamped ends. An interesting development of the J-Q trajectories is shown in Fig. 2(a) for the deep crack specimen ($a/W = 0.5$) with pin-loaded ends. While the J-Q curves for $H/W = 4$ and 6 remain very similar, the specimen with $H/W = 2$ responds essentially the same as a deep notch C(T) specimen [4].

3.2 Fracture Behavior of SE(T) Specimens and Cracked Pipes

Figures 3(a-b) compare the evolution of parameter Q with crack-tip loading (as measured by J) for the pin-loaded and clamped SE(T) specimens with $H/W = 6$ against the cracked pipe with $D = 508$ mm (20 in). The analyses consider equal relative crack sizes for the SE(T) specimens and cracked pipes, a/W and $a/t = 0.1$, 0.25 and 0.5. In all plots, Q is defined by Eq. (2) at the normalized distance ahead of crack tip given by $r = 2J/\sigma_0$ whereas J is normalized by $b\sigma_0$ with b denoting the remaining crack ligament $W - a$ (fracture specimen) or $t - a$ (cracked pipe). Figure 3(a) clearly demonstrates the effectiveness of the pin-loaded SE(T) specimens to characterize cleavage fracture in the cracked pipes for the entire range of crack sizes, particularly for medium and short crack sizes ($a/t = 0.1$, 0.25). J-Q trajectories for the deep crack configurations (a/W and $a/t = 0.5$) display somewhat larger differences (compared to other analyzed crack configurations) for higher J-values but which can still be considered reasonably close. In contrast, Fig. 3(b) reveals that the J-Q curves for the clamped SE(T) specimens with $a/W = 0.5$ differ significantly from the corresponding curves for the cracked pipe with $a/t = 0.5$. However, the clamped SE(T) specimens with medium and short crack sizes ($a/W = 0.1$, 0.25) exhibit J-Q trajectories which are close to the corresponding curves for the cracked pipes ($a/t = 0.1$, 0.25).

4 CONCLUDING REMARKS

This study presents non-linear, plane-strain analyses of fracture specimens and axially cracked pipes

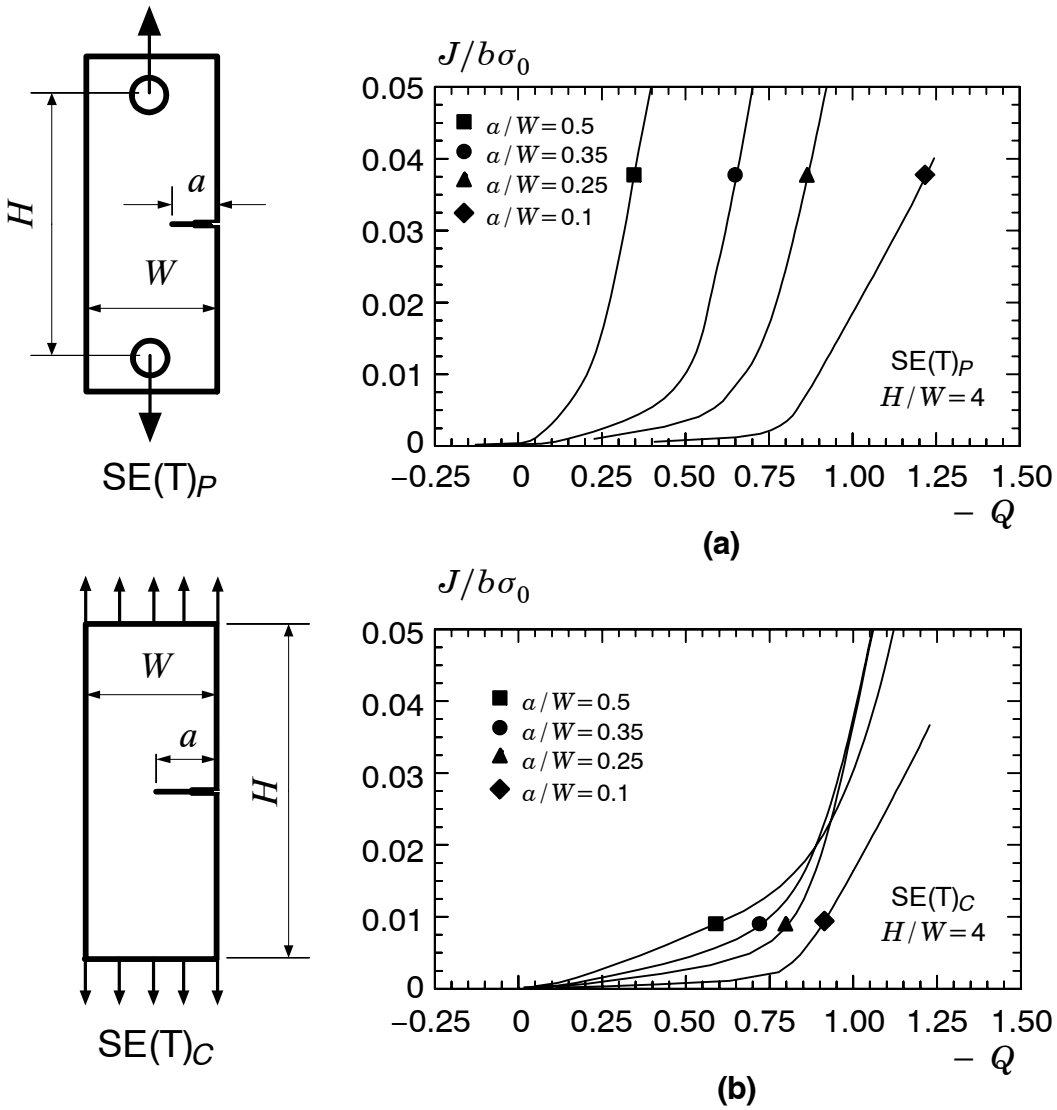

Figure 1 *Effect of loading condition on J-Q trajectories for the SE(T) specimens with H/W = 4 and n = 10 material: (a) Pin-loaded specimens and (b) Clamped Specimens.*

which reveal strong effects of geometric parameters (a/W, H/W and a/t-ratios) and loading conditions on crack-tip constraint. These analyses demonstrate that pin-loaded SE(T) specimens provide crack-tip conditions which are essentially similar to axially cracked pipes with identical (relative) crack depths, particularly for moderate to shallow crack sizes. Clamped SE(T) specimens with short cracks also display levels of crack-tip constraint which are similar to corresponding axially cracked pipes, but the crack-tip driving forces for these specimens with deep cracks differ widely from crack-tip driving forces for cracked pipes with axial deep flaws. Overall, the pin-loaded SE(T) specimens

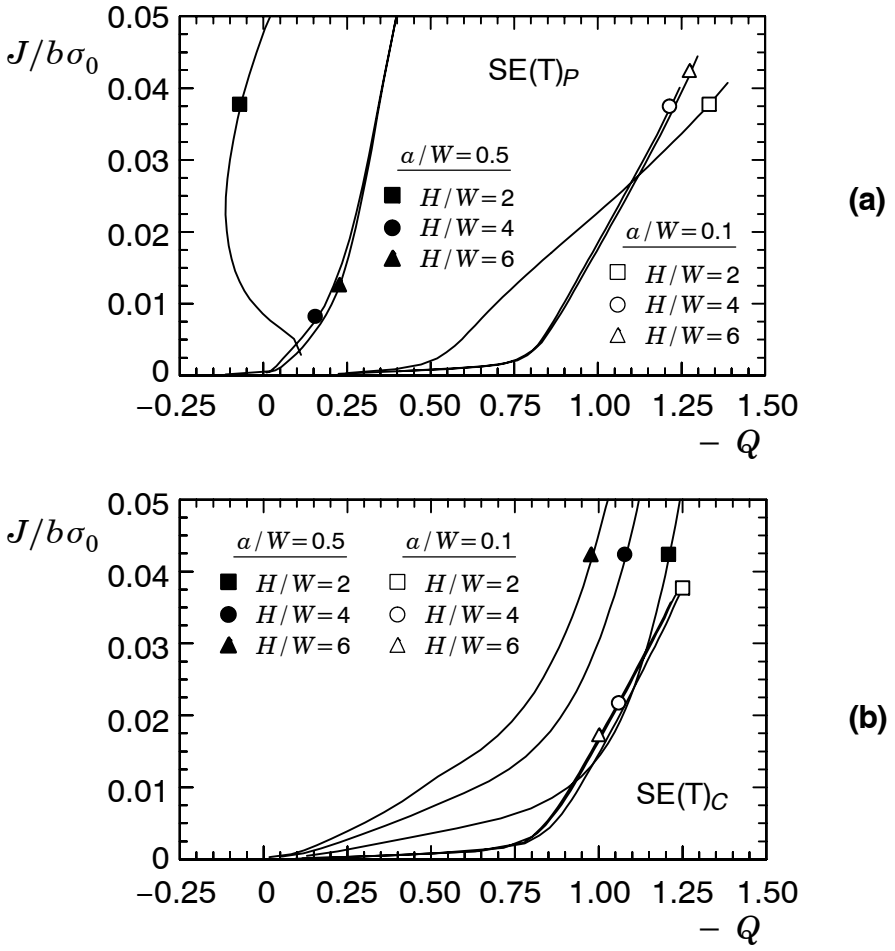

Figure 2 *Effect of loading condition on J-Q trajectories for SE(T) specimens with n = 10 ($E/\sigma_0 = 500$) and varying H/W-ratios: (a) Pin-loaded specimens and (b) Clamped Specimens.*

appear to provide a better description of axially cracked pipes. While the plane-strain analyses conducted here do not address 3D effects (thereby not including the coupling between in-plane and through-thickness effects on crack-tip fields), the results encourage further investigations in the development and utilization of constraint-designed SE(T) specimens in fracture assessments of pressurized pipes and cylindrical vessels.

Acknowledgments

This investigation is supported by Fundação de Amparo à Pesquisa do Estado de São Paulo (FAPESP) through Grant 03/02735-6 and a graduate scholarship (02/06328-3) provided to the first author (SC). Funding to the second author (CR) is also provided by Conselho Nacional de Desenvolvimento Científico e Tecnológico (CNPq).

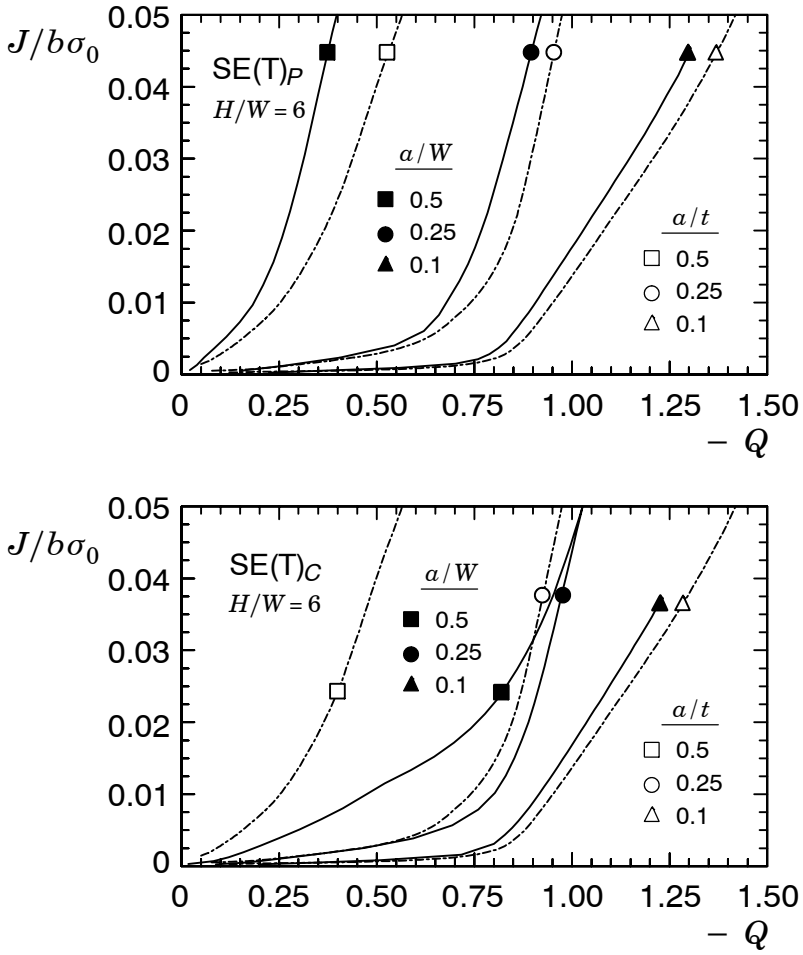

Figure 3 *J-Q trajectories for SE(T) specimens with H/W = 6 and cracked pipes with D = 508 mm (20 in) for n = 10 and varying crack sizes: (a) Pin-loaded specimens; (b) Clamped Specimens*

REFERENCES

[1] O'Dowd, N.P., and Shih, C.F., "Family of Crack-Tip Fields Characterized by a Triaxiality Parameter: Part I - Structure of Fields," *Journal of the Mechanics and Physics of Solids*, Vol. 39., No. 8, pp. 989-1015, 1991.

[2] O'Dowd, N.P., and Shih, C.F., "Family of Crack-Tip Fields Characterized by a Triaxiality Parameter: Part II - Fracture Applications," *Journal of the Mechanics and Physics of Solids*, Vol. 40, pp. 939-963, 1992.

[3] Koppenhoefer, K., Gullerud, A., Ruggieri, C., Dodds, R. and Healy, B. "WARP3D: Dynamic Nonlinear Analysis of Solids Using a Preconditioned Conjugate Gradient Software Architecture." *Structural Research Series (SRS) 596*. UILU-ENG-94-2017. University of Illinois at Urbana-Champaign. 1994.

[4] Cravero, S. and Ruggieri, C. "Assessments of Cleavage Fracture in High Pressure Pipelines with Axial Flaws Using Constraint Designed Test Specimens - Part I: Plane-Strain Analyses", Submitted for Publication.